SCIENTIFIC HIGHLIGHTS

Index

DIPC Highlight

Understanding Biological Photoreceptors

by *M.A.L. Marques[1], X. López[2], D. Varsano[1,3], A. Castro[4,3] and A. Rubio[1,3,5]*

We have implemented a new scheme to describe the photoresponse and structural dynamics of bio-photoreceptors. The scheme can shed light into the initial microscopic origin of vision, photosyntesis and bacteria luminiscence processes.

Chromophore isomerisation is at the heart of biomolecular photophysics.

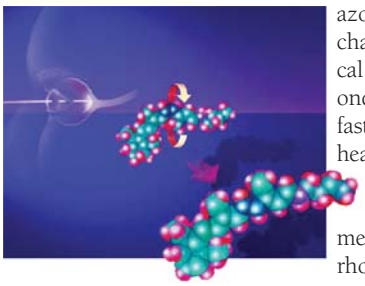

One of the most fundamental, intriguing and relevant bio-physical process is the microscopic description of the photo-response of bio-molecules. From the photosynthesis to the human vision processes, DNA damage and bacteria bio-luminescence; those phenomena require an understanding of how light is absorbed and how that energy is transfer from the photoreceptor sites to the active biological centers. A famed organic molecule is the azobenzene chromophore, (formed by joining two phenyl rings with the azo group) that undergoes a structural change (cis/trans-isomerization) under optical irradiation, and it does so in a femtosecond time-scale. These light-induced ultra fast rotations around double bonds are at the heart of most photo-active bio-organic reactions. In particular the first step of the human vision are related to cis/trans isomerization of the retinal chromophore of rhodopsin (see figure). The induced structural transformation upon light absorption is very fast (few hundred femtoseconds; 1fs=10^{-15}s) and is associated to the presence of ring structures in the molecule (as benzene or imidazoline groups).

The cited phenomena involve i) different energy (from covalent to van der Waals bonding) and time scales (from fs for the electron dynamics, to ps for the ionic motion and ms for structural reorganizations); ii) light-induced chemical reactions that are intrinsically non-adiabatic, and require techniques that go beyond the traditional Born-Oppenheimer separation of electronic and nuclear degrees of freedom. Therefore, there is a clear need for a reliable theoretical framework to describe processes related to the excited-state dynamics of biological complexes either in vacuo or in solution. In 2002 we joined efforts with the theoretical quantum chemistry group to set up an ambitious project with the goal of developing a theoretical scheme able to predict the photo-induced dynamics in bio-molecular structures. We present here the first results noticing that many other fascinating results are just coming up. Our approach is based on a divide-and-conquer strategy where the active part of the structure is fully described microscopically using quantum mechanics schemes, whereas the environment (i.e., rest of the protein, membrane and solvent) is described using a classical molecular mechanics method (QM/MM approach). The novelty of our work is the simulation of the combined electron-ion dynamics of the photoreceptor within the framework of time-dependent density functional theory (TDDFT). By solving a set of coupled time-dependent Schrödinger-like equations (including light sources as short laser pulses), we identify the mechanisms active at the different time-scales of the photo-process.

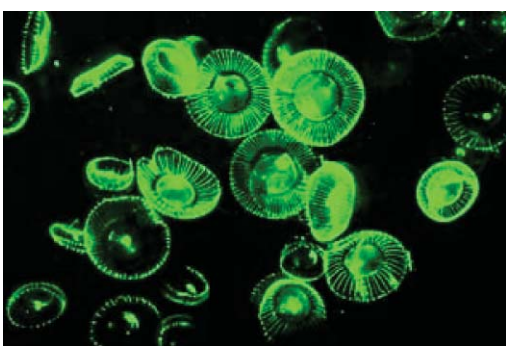

1 Departamento de Física de Materiales, UPV/EHU, San Sebastián, 2 Departamento de Química, UPV/EHU, San Sebastián, 3 Donostia International Physics Center, San Sebastián, 4 Departamento de Física Teórica, Universidad de Valladolid, Spain, 5 Centro Mixto CSIC-UPV/EHU, San Sebastián

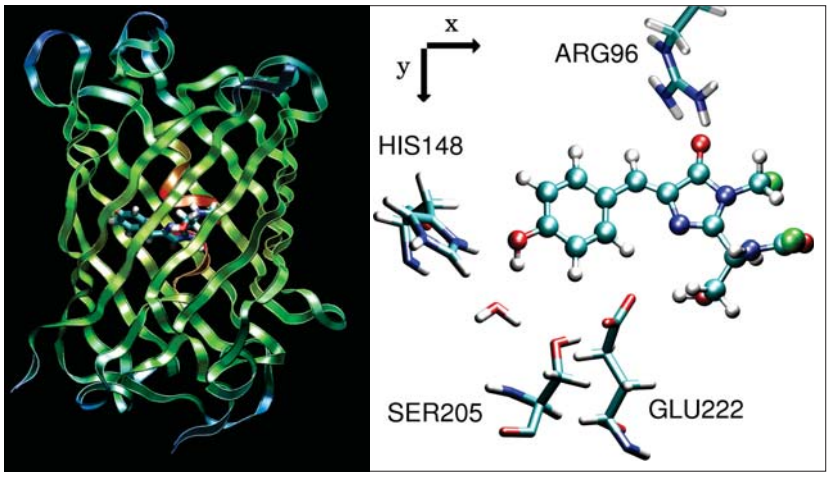

In this context, the Green Fluorescent Protein (GFP) has become a unique tool in molecular biology because of its fluorescent properties and inertness when attached to other proteins. The optical absorption spectrum of the wild type (wt)-GFP, measured at 1.6 K, shows two main resonances at 2.63 and 3.05 eV that are attributed to the two thermodynamically stable protonation states of the chromophore (negative and neutral configurations, respectively). Excitation at either frequency leads to fluorescent green-light emission, peaked at 2.44eV, which is the main mechanism for energy release in wt-GFP. This internal photo-conversion process occurs very rapidly by excited-state proton transfer for the neutral chromophore. The photo-physics of the GFP is governed by a complex equilibrium between the neutral and anionic configurations. Thus, GFP is the ideal system to test our theoretical approach. First we determined the structure of the GFP and then computed the photo-absorption cross section for visible light as it has to be properly described before we could dream of describing any dynamical process.

The GFP protein is folded in a b-sheet barrel conformation with the cromophore occupying a central position inside the barrel (see figure). The cromophore is formed by two consecutive rings, the phenol-type ring of Tyr66 and a five member heterocyle formed by the backbone of Tyr66, the carbonyl carbon of Ser65 and the nitrogen of the backbone of Gly67. The theoretical photo-absorption cross-section is compared to the experiments in the figure (the dashed line corresponds to the neutral chromophore, the dotted line to the anionic, whereas the green and blue curves are the experimental results of S.B. Nielsen et al, PRL87, 228102 (2001) and of T.M.H. Creemers et al, PNAS 97, 2974 (2001), respectively). The strength of the main p - p* transition is larger in the anionic than in the neutral GFP. It is, however, possible to obtain a quantitative description of the spectra of the wt-GFP by assuming a 4:1 ratio for the concentration of the neutral/anionic forms. This value is very close to the estimated experimental ratio of 80% neutral and 20% anionic. Besides the good description of experiments we noticed that GFP is a rather anisotropic molecule in the visible (see inset in the figure). Only light polarized along the pentagon-hexagonal ring is absorbed with high yield. This property can be used to enhance the photo-dynamical processes of GFP samples for opto-electronic devices, e.g. depositing well oriented GFP molecules on top of doped-semiconductor substrates we could get photovoltaic structures with high efficiency.

We have shown that a combined QM/MM and TDDFT approach is able to reproduce the optical response of the GFP. This is a major step toward the first-principles description of excited-state dynamic of important biological photo-receptors. Transient and time-resolved optical spectroscopy could be studied. However, in spite of the good agreement, some questions remain open. For example, how does the excitation in the GFP trigger the proton shuttle mechanism and what is the time-scale for this process? To answer these questions we have to go beyond the present work including the excited state dynamics of the environment (e.g. the proton-transfer involves structural modifications of the environment that have to be properly described). Work along this line is in progress. ■

Our TDDFT approach constitutes a major step towards the first principles description of the combined electron/ion dynamics in bio-photoreceptors.

REFERENCE
M.A.L. Marqués, X. López, D. Varsano, A. Castro and A. Rubio, Physical Review Letters **90**, 258101 (2003)

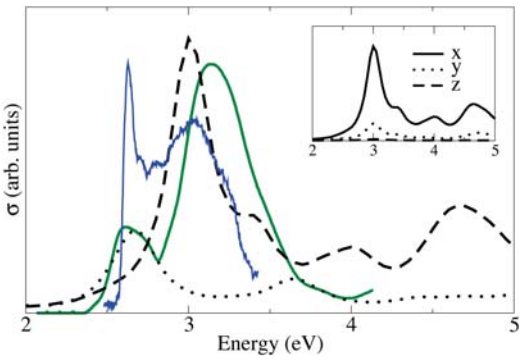

DIPC Highlight

Mixing One-dimensional Cold Atomic Gases

by *M.A. Cazalilla*[1] *and A.F. Ho*[2,1]

Just as mixing two fluids (e.g. water and oil) under certain conditions of temperature and pressure can lead to a variety of phenomena, mixing two types of cold atomic gases confined to one-dimension can lead to a number of interesting quantum phenomena. This includes the usual demixing (like the one observed at room temperature and pressure between oil and water), collapse, or more interestingly the formation of "pairs" of atoms of different species that are correlated over long distances.

The large tunability of cold atomic gases allows to study interesting many body phenomena.

Ever since the achievement of Bose-Einstein condensation of a dilute gas of alkali (Rubidium) atoms in the summer of 1995, the field of cold atomic gases has made astonishing experimental progress. The ultimate goal has become to learn how to manipulate cold atomic gases to realize exotic phases of matter. The latter may find applications in quantum information processing and storage. It is also expected that they can provide us with new and key insights into the physics of quantum many-body systems that may help us understand some of the puzzling behaviour of the high-Tc copper-oxide superconductors and other exotic materials.

One dimensional systems of cold atoms have only recently become available, and are very interesting because of the strong enhancement of correlations as the dimensionality of the system decreases. So far, most experiments are made with bosonic atoms (like ^{87}Rb) confined by very anisotropic potentials. However, not far in the future fermions (like ^{6}Li) will also be used. Bosons confined to one dimension (1D) are interesting per-se, as there are not many realizations of these systems in Nature (apart from spins in highly anisotropic magnetic materials).

A single-component gas of cold bosons, when confined to 1D, will not undergo Bose-Einstein condensation since all possible fluctuations must propagate on a line and any kind of ordering (like Bose-Einstein condensation) will be strongly suppressed. However, in the finite-size systems of experimental interest, phase coherence can be approximately maintained over many times the average atom-atom distance so that these systems resemble very much a Bose-Einstein Condensate (BEC). This is why they are frequently called quasi-condensates. However, if the strength of the interactions is increased, the (phase) fluctuations are enhanced and the system will not behave as a condensate anymore. This is the case as the extreme limit where no boson can pass each other (i.e. the bosons become "hard core") is approached. A gas of hard-core bosons is known in the jargon of the field as a Tonks gas, in honor of Lewi Tonks, who first discussed the properties of a classical gas of hard-core particles in 1936. Between the Tonks gas limit and the quasi-condesate, the system exhibits a rather smooth crossover, and no new phenomena are expected.

On the other hand, when a two-component 1D gas is considered (a binary mixture), the

1 Donostia International Physics Center, San Sebastián 2 School of Physics and Astronomy, University of Birmingham, Edgbaston, U.K.

resulting system exhibits a much richer and interesting behaviour. First of all, just like with ordinary (classical) fluids, the system can demix (like oil and water do at room temperature and pressure) if the two components repel sufficiently strongly, or it can collapse if they attract sufficiently strongly. However, the quantum nature of this matter leaves room for more surprises.

In 1974 two American theoretical physicists stumbled upon a particular type of one-dimensional matter. When opposite-spin electrons attract in a one-dimensional metal they could form pairs. The analogy with the so-called Cooper pairs, discovered by Leon Cooper in 1957, and which eventually would be instrumental for understanding the mechanism of superconductivity in conventional superconductors (like lead or aluminum), was unavoidable. However, as Luther and Emery cleverly pointed out, fluctuations would never allow the electron-pairs to condense (as Cooper pairs do in superconductors), and therefore establish a macroscopic phase coherence throughout the system. That is why the system would exhibit a gap only to spin excitations and would remain gapless for charge excitations. In contrast, in higher dimensional materials condensation of Cooper pairs opens a gap to all excitations, both spin and charge, and only in neutral systems (like in Helium 3) one can have a gapless collective mode known as the Anderson-Bogoliubov mode. All in all, the model was the closest thing to a higher dimensional superconductor that one can get in one dimension, and it goes under the name of Luther-Emery liquid.

Remarkably, we found that the phenomenon discovered by Luther and Emery can also take place in a binary mixture of two cold atomic gases. In our letter, we studied two types of these systems, depending on the statistics of the components. Thus if the two components are bosonic, we termed the mixture of B+B type, whereas it one of the components is a boson and the other is a fermion, we termed it of B+F type. We found that if the bosons of the same type repel each other very strongly, i.e. if they are driven into the Tonks gas regime, and provided the number of particles of each species and the velocity are equal and different species attract, they could form the same type of pairs that Luther and Emery found for a one-dimensional metal where electrons attract each other.

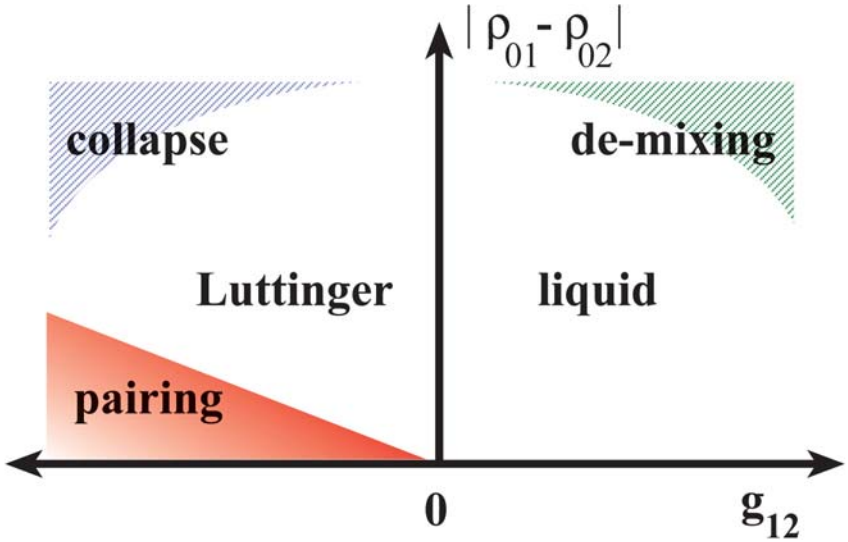

Schematic phase diagram with the boson(s) in the Tonks limit. $|\rho_{01} - \rho_{02}|$ is the density difference

In a mixture of a boson and a fermion, this has interesting consequences, the pair (the "composite fermion") will behave as a fermion and therefore carries a finite momentum which is of the order of the Fermi momentum. This is somewhat analogous to the condensation of Cooper pairs at finite momentum that takes place in certain superconductors under the influence of a strong magnetic field (the so-called Fulde-Ferrell-Larkin-Ovchinnikov state). However, the analogy cannot be pushed too far, because in contrast to the latter systems, the composite fermions would never condense even in higher dimensions due to their statistics. In 1D however, for sufficiently strong attraction between the boson and the fermion, the gas of composite fermions would still acquire some superfluid properties. ■

We have found an exotic phase where atoms of two difference species pair up in a strongly correlated cold atomic gas confined to move in one dimension

REFERENCE
M. A. Cazalilla and A. F. Ho, Physical Review Letters **91**, 150403 (2003)

DIPC Highlight

Role of Bulk and Surface Phonons in the Decay of Metal Surface States

by *A. Eiguren[1], B. Hellsing[2], F. Reinert[3], G. Nicolay[3], E. V. Chulkov[1,4], V. M. Silkin[4], S. Hüfner[3] and P. M. Echenique[1,4]*

Understanding the temporal evolution of quasiparticles (electron and holes) on metal surfaces is of paramount importance to describe many important phenomena such as the dynamics of charge and energy transfer, quantum interference, and localization. Typically, the quantity used to characterize this temporal evolution is the lifetime, which refers to the time the quasiparticle retains its identity. It is the interaction of the quasiparticle with the metal (electrons, phonons...) what makes the lifetime finite. We present the first microscopic analysis of the electron-phonon mechanism and find that its contribution, together with the electron-electron mechanism, is crucial in order to understand the experimental lifetime of the sp surface state on Cu (111) and Ag (111).

Electron-phonon interaction gives important contribution to electron (hole) dynamics on metal surfaces and controls temperature dependence of this dynamics.

The sp surface state in the L-gap of the (111)-surface of noble metals forms a two-dimensional (2D) electron gas and the electron-electron (e-e) contribution to the hole lifetime has been rationalized in terms of a dominant contribution from intraband transitions within the 2D surface state band, screened by the underlying 3D bulk electron system, and in terms of interband transitions (bulk states $\rightarrow$ surface state) (Science, 288, 1399 (2000)). However, an appropriate calculation of the electron-phonon (e-p) contribution to the lifetime broadening of surface states has not been done yet. Many properties of metals, such as resistivity, specific heat, and superconductivity, reflect the importance of the e-p interaction. The strength of this e-p coupling is usually measured in terms of a parameter λ that depends on the energy and momentum involved in the process under consideration. We have presented a theoretical analysis of the e-p contribution to the lifetime broadening of surface electron states, taking into account all electron and phonon states involved in the e-p scattering process. The theoretical analysis is based on a calculation of the full Eliashberg spectral function, which enables us to resolve, in detail, the contributions from different phonon modes, as well as, the general temperature dependence. Including the e-e interaction, our theoretical results are compared with new energy and temperature dependent high-resolution photoemission data.

In Fig.1 the calculated temperature dependent e-p contribution (solid lines) to the lifetime broadening Γ together with e-e contribution Γ_{ee} (dotted lines) is compared with the measured temperature dependence of Γ (circles) for Cu (111) and Ag (111). The insert shows the measured energy distribution curves for Cu (111) for selected temperatures.

1 Departamento de Física de Materiales and Centro Mixto CSIC-UPV/EHU, San Sebastián **2** Department of Physics, Chalmers University of Technology and Göteborg University, Sweden **3** Fachrichtung Experimentalphysik, Universität des Saarlandes, Saarbrücken, Germany **4** Donostia International Physics Center, San Sebastián

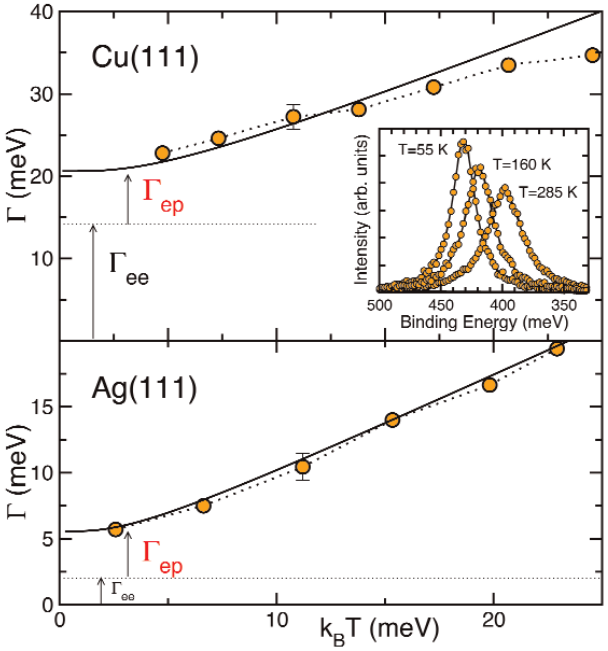

Fig.1. Temperature dependence of the lifetime of the sp surface state

Surface phonon modes are crucially important for the description of electron dynamics on surfaces.

In Fig.2 the calculated Γ_{ep} (red lines) as well as Γ_{ee}+ Γ_{ep} (black lines) are shown for Cu (111) and Ag (111) together with the experimental results (diamonds) as a function of energy at T=30K. As follows from Fig. 2, the contribution from only the Rayleigh mode (blue lines) gives about 40% of Γ_{ep} beyond the maximum phonon frequencies, indicating that bulk phonons give most of the contributions in this range. But for binding energies below the maximum of the Rayleigh mode energy, this mode alone represent on average about the 85% of Γ_{ep}.

Detailed comparison of the theoretical results with photoemission data (this work and Phys. Rev. B 63, 115415 (2001)) as well as with scanning tunnelling spectroscopy results (Science, 288, 1399 (2000)) shows an excellent agreement between the theory and experiments that opens new perspectives in investigations of dynamical processes on clean metal surfaces as well as on surfaces with adatoms and adlayers at different temperatures. ■

REFERENCE
A. Eiguren, B. Hellsing, F. Reinert, G. Nicolay, E. V. Chulkov, V. M. Silkin, S. Hüfner and P. M. Echenique, Physical Review Letters **88**, 066805 (2002)

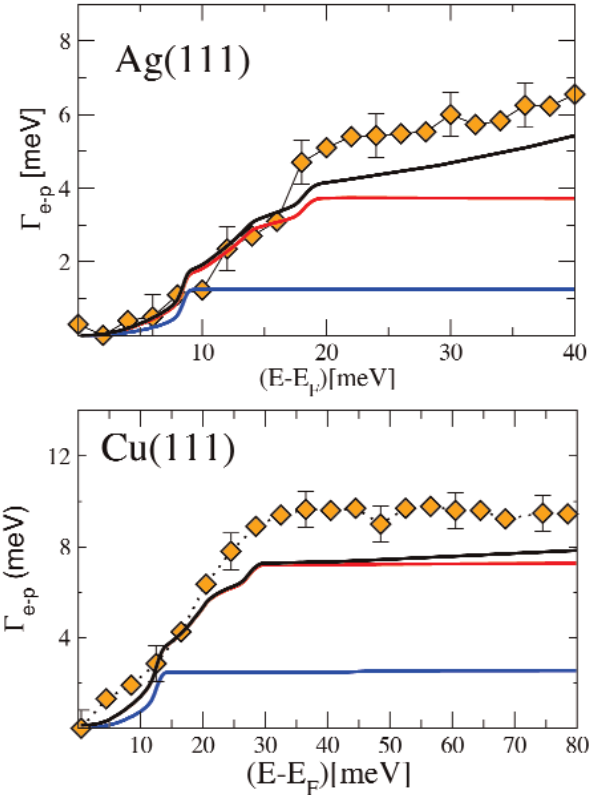

Fig. 2. Lifetime broadening of the electron state depending on its binding energy

DIPC Highlight

Cherenkov Effect in Photonic Crystals

by *F. J. García de Abajo*[1], *A.G. Pattantyus-Abraham*[2], *N. Zabala*[1,3], *A. Rivacoba*[1,4], *M.O. Wolf*[2], *and P. M. Echenique*[1,4]

Like the wake produced by a boat moving faster than surface waves in a quiet lake, fast electrons moving faster than light in a dielectric produce the so-called Cherenkov radiation, which leads ultimately to stopping of the projectiles.
This effect has been observed for electrons traversing photonic crystals, where light is subject to a periodically modulated dielectric constant and allowed to propagate within so-called photon bands, similar to electronic bands in solids. The electrons lose energy to produce photons with probability proportional to the local density of the photonic states at the position of the electron beam. This permits us to map photonic bands by observing the energy and angle distribution of the transmitted electrons.

Cherenkov light can reflect how photons propagate in photonic crystals.

Light can be slowed in matter so that charges traveling faster that it may lose part of their energy to produced a cone of Cherenkov light emission, similar to the wake of a boat moving faster than surface waves in water. The same phenomenon can take place if the charges move inside a photonic crystal, where light is subject to propagation only along certain directions for given frequencies, and the resulting light emission must reflect the complexities of the photonic band structure in these materials.

Our group, working in collaboration with Dr. Andras Pattantyus and Dr. Michael Wolf of the University of British Columbia (Canada), have managed to prove this effect by observing energy losses in fast electrons transmitted through pores drilled in 1-micron thick alumina films. The transmitted electrons exhibited a marked tendency to lose energy in the 7-8.5 eV region, depending on the velocity of the electrons and in good agreement with calculations of light emission proba-

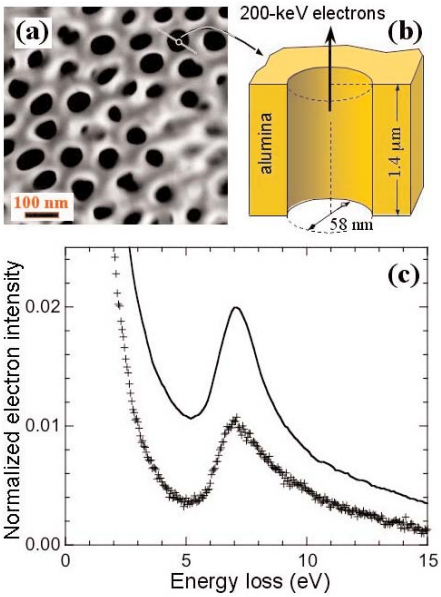

Fig. 1. Cherenkov losses in a photonic crystal

1 Centro Mixto CSIC-UPV/EHU and Donostia International Physics Center, San Sebastián 2 Department of Chemistry, University of British Columbia, Vancouver, Canada 3 Departamento de Electricidad y Electrónica, UPV/EHU Bilbao, Spain 4 Departamento de Física de Materiales, UPV/EHU, San Sebastián

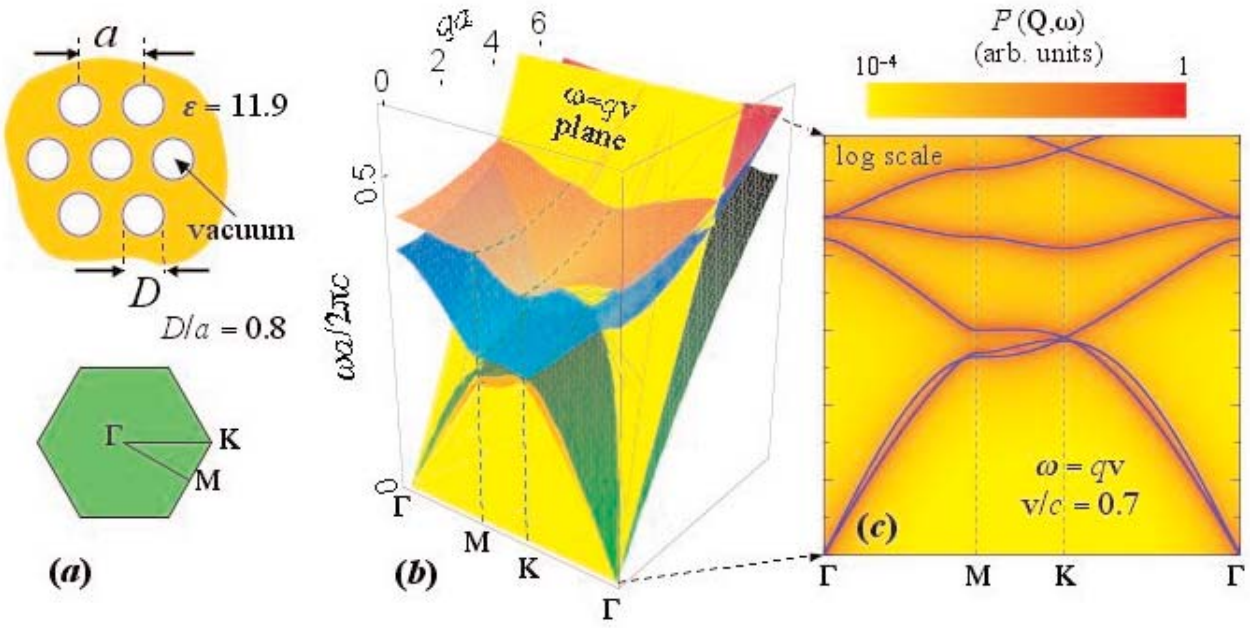

Fig. 2. Mapping photonic bands with fast electrons

bility, which is more pronounced at those energies. The electrons were made to pass through the holes without actually touching the material, and the fact that alumina is transparent across distances of several microns at those photon energies led the researchers to conclude that the observed energy losses must arise from Cherenkov light emission. More precisely, Fig. 1 shows a transmission electron microscope image of a porous alumina film (a), a schematic view of one of the holes showing the electron trajectory (b), and the distribution of electrons as a function of the energy that they have lost (c), theory (symbols) compared with experiment (curve), with clear evidence of the Cherenkov effect (7 eV peak).

Unlike Cherenkov emission in a homogeneous medium, the restriction imposed by a 2D patterning of holes in the alumina films limited this emission to within the abovementioned energies. Further analysis of the bending in the trajectory of the electrons can provide a basis for direct mapping of photonic bands by fast electrons, theory suggets (see Physical Review Letters 91, 143902, 2003), as shown in Fig. 2, that depicts a schematic diagram of a two-dimensional crystal made of cylindrical holes, along with its first Brillouin zone (a), the band structure of this crystal and its variation with light momentum parallel to the cylinders q (b), and a cut of the bands along the **ω=**qv plane (c). Electrons moving with velocity v along the cylinders can only sense photonic states that satisfy this condition. The underlying density plot in (c) shows the probability that the electrons lose a certain amount of energy w with their trajectory is deflected by a given momentum within the first Brillouin zone. ■

Photonic bands are mapped by energy and angle distributions of fast electrons transmitted through photonic crystals.

REFERENCE

F. J. García de Abajo, A. G. Pattantyus-Abraham, N. Zabala, A. Rivacoba, M. O. Wolf, and P. M. Echenique, Physical Review Letters **91**, 143902 (2003)

DIPC Highlight

Interplay of Surface Plasmons and Image States

by *A. García-Lekue[1], J.M. Pitarke[1,2], E.V. Chulkov[2,3], A. Liebsch[4] and P.M. Echenique[2,3]*

Our investigations on the combined effect of single-particle and collective surface excitations in the decay of image-potential states on Ag surfaces provide new insight to elucidate the origin of the long-standing discrepancy between experimental measurements and previous theoretical predictions for the lifetime of these states. Although surface-plasmon excitation had been expected to reduce the image-state lifetime, we have demonstrated that the subtle combination of the spatial variation of s-d polarization in Ag and the characteristic non-locality of many-electron interactions near the surface yields surprisingly long image-state lifetimes, in agreement with experiment.

The coupling of excited states with the solid governs the cross sections and branching ratios of practically all electronically induced adsorbate reactions at metal surfaces.

Fundamental concepts in condensed matter physics are those of surface plasmons and image states. Surface plasmons, which are quanta of collective oscillations of electrons at metal surfaces, crop up in a number of scenarios from electron energy loss to the colourful appearance of suspensions of small metallic particles, surface-plasmon resonance technology, and a wide range of photonic applications. Image states are quantized electronic states that are observed outside certain metal surfaces due to the attractive image potential that occurs between the electron and the solid. Image states dynamics provides insight into the investigation of the coupling of excited surface electronic states with the underlying substrate. This coupling of these states with the underlying substrate is known to govern the cross sections and branching ratios of practically all electronically induced adsorbate reactions at metal surfaces.

In most metals, there is no interplay between surface plasmons and image states, which is due to the fact that the surface-plasmon energy is typically too large for image states to couple with them. In silver, however, the presence of occupied narrow bands of d electrons considerably reduces the surface-plasmon energy, and the relaxation of image states via the creation of surface collective excitations becomes feasible in this material.

The broadening (and therefore finite lifetime) of the first (n=1) image state at the Γ point on the Ag(100) surface mainly originates in processes in which the image-state electron with an energy of 3.9 eV above the Fermi level decays into an empty state with energy still above the Fermi energy. These processes can be realized by transferring energy and momentum to an excitation of the medium, thereby creating either an electron-hole pair or a collective surface excitation of energy smaller than 3.9 eV. The energy of surface plasmons in Ag is 3.7 eV.

The inelastic broadening of excited states in solids can be obtained from the projection (over the excited state wavefunction) of the imaginary part of the so-called electron self-energy of many-body theory, which accounts for the many-body interactions in the solid. Following this formalism, we have investigated the decay of the Ag (100) n=1 image state by treating Auger-like single-particle and collective surface excitations on the same footing. A consistent treatment of these decay channels is particularly important because of the near-degeneracy of the image state energy with the Ag (100) surface plasmon.

The surprising and novel result of our work is that, although the imaginary part of the image-state self-energy is enhanced due to the presence of the plasmon decay channel, interferences resulting from the non-locality

1 Departamento de Física de Materia Condensada, UPV/EHU, Bilbao, Spain **2** Centro Mixto CSIC-UPV/EHU and Donostia International Physics Center, San Sebastián **3** Departamento de Física de Materiales, UPV/EHU, San Sebastián **4** Institut für Festkörperforschung, Forschungszentrum Jülich, Germany

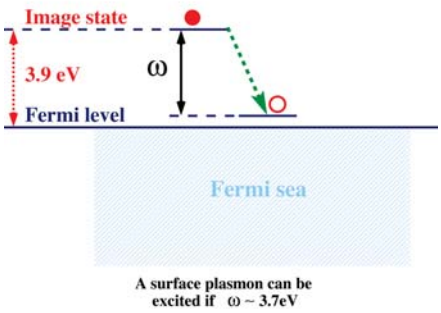

Energetic diagram of the decay of the first Ag (100) image state

of the self-energy lead to a smaller overall image-state broadening, in agreement with experiment. This elucidates the origin of the long-standing discrepancy between experimental measurements and previous theoretical predictions for the lifetime of these states.

First-principles descriptions of electron dynamics in the bulk of noble metals show that deviations from electron dynamics in a gas of sp electrons mainly originate in the participation of d electrons in the screening of electron-electron interactions. Hence, in order to avoid the use of too-expensive ab initio techniques at the noble metal surface Ag (100), the approach we have undertaken is based on (i) the use of a physically motivated one-dimensional potential which accurately accounts for the dynamics of sp valence electrons, and (ii) the replacement of occupied d bands in Ag by a polarizable medium giving rise to additional screening. We emphasize that our approach provides a coherent treatment of single-particle and collective surface excitations.

The n=1 image-state wave function on Ag (100) (dotted line in the figure, where z is the coordinate normal to the surface) has a maximum at a few angstroms outside the crystal edge (z=0), which we choose to be located half a lattice spacing beyond the last atomic layer. The solid line in the figure shows the imaginary part of the n=1 image-state self-energy (this nonlocal quantity Im[-Σ] couples the coordinates z and z') versus z for a fixed value of z' outside the solid (red circle). We note that the main peak of Im[-Σ] does not occur at z=z', as would be the case in the interior of the solid; instead, it lags behind and remains localized near the surface where the image-state wave function is negative. Consequently, there is a major interference contribution to the projection of Im[-Σ] over the image-state wave function, which is negative and yields a large reduction of the image-state broadening.

The role that the screening of d electrons plays lowering the surface-plasmon energy, and therefore opening a new coupling of image states with the solid, is particularly pronounced on the vacuum side of the surface, where negative interference dominates. Hence, the combined effect of decay via surface plasmons and nonlocality of the self-energy is a considerably reduced lifetime broadening. While in the absence of d electrons the broadening of the n=1 image state on Ag (100) would be 18 meV, our theory (with d electrons and surface-plasmon decay included) yields a broadening of 12 meV (i.e., a lifetime of 55×10^{-15}s) in excellent agreement with recently reported time-resolved two-photon photoemission (TR-2PPE) measurements. ■

Despite the enhancement of the image-state self-energy in Ag due to the decay via surface plasmons, the highly nonlocal character of the self-energy in the surface region ultimately leads to a surprisingly small lifetime broadening, in agreement with experiment.

REFERENCE
A. García-Lekue, J. M. Pitarke, E. V. Chulkov, A. Liebsch, and P. M. Echenique, Physical Review Letters **89**, 096401 (2003)

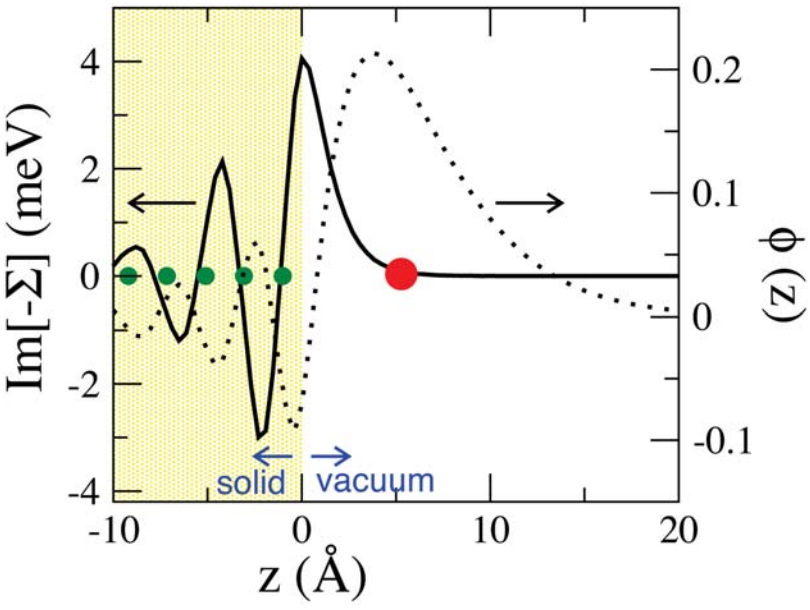

Wave function and imaginary part of the n=1 image state self-energy

DIPC Highlight

Nonlinear Screening in Two-Dimensional Electron Gases

by *E. Zaremba*[1,2], *I. Nagy*[3,2], *and P.M. Echenique*[4]

A charged impurity or projectile inmersed in a metal induces the rearrangement of the electrons around it, providing the total screening of the charge. Typically, the impurity represents such a strong perturbation that a nonlinear screening theory is needed to account for the modifications of the local electronic structure. The possible realization of quasi-two-dimensional systems in a variety of contexts (semiconductor heterostructures, electrons on the surface of liquid helium, layered materials...), has led us to study the screening of a point charge in a *two-dimensional* electron gas using a *density functional method*. In marked contrast to the three-dimensional case, we find that the screened potential for a proton supports a bound state even in the high-density limit.

In the high density limit, the screening density in a two-dimensional electron gas is simply proportional to the perturbing potential.

Today condensed matter physics is by far the largest field of physics. It is concerned with the study of solids. A subtle task considering the huge number of particles one has to deal with (a mollar quantity of a solid contains as many as 10^{23} atoms). Different theories have been developed in finding approximations to handle this problem. Among them, modern density-functional theory (DFT) makes two kinds of contribution to the science of multiparticle quantum systems. The first is in the area of fundamental *understanding*, since DFT focuses on quantities in the real coordinate space, principally on the electron density n(r). This quantity, similarly to the exchange-correlation hole density, is physical and transparent. Their understanding provides a complementary insight into the nature of multiparticle systems. The second contribution is *practical*. The theory leads to self-consistent field equations, similar to the Hartree equations, in which the effects due to the interparticle Coulomb interaction and the Pauli exclusion principle are included by addition of the exchange-correlation potential.

The capability of this practical mapping between the real, interacting many-electron system and an idealized system of noninteracting electrons moving in an effective single-particle potential, still remained as a nontrivial question for reduced dimensions. The possible realization of two-dimensional (2D) electron systems in a variety of context (semiconductor heterostructures, image or band-gap surface states at metal surfaces, and layered materials) confirms the relevance of this question. In all these cases, the interaction of external charges with the two-dimensional electron gas (2DEG) is a problem of both fundamental and practical interest. Experimentally, the powerful scanning tunneling microscopy offers a direct means of determining the modulated electron density through the observation of induced Friedel oscillations. Furthermore, transport of elec-

1 Department of Physics, Queen's University, Kingston, Ontario, Canada 2 Donostia International Physics Center, San Sebastián 3 Department of Theoretical Physics, Technical University of Budapest, Hungary
4 Departamento de Física de Materiales and Centro Mixto CSIC-UPV/EHU, San Sebastián

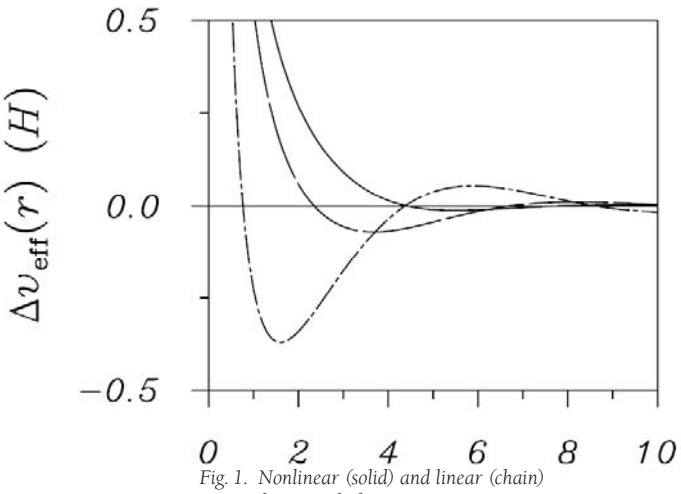

Fig. 1. Nonlinear (solid) and linear (chain) screened potentials for an antiproton

trons is often limited in real matter by impurity scattering and, thus, a detailed knowledge of the scattering potential is also needed. All these reasons motivated us to investigate within the context of DFT, the nonlinear screening of a point charge, Z, located in the plane of a 2DEG.

As is the case in 3D, the screening potential of a negatively charged impurity (an antiproton, for instance) repels electrons almost completely from the charge, leaving exposed the positive background of the metal, which neutralizes the impurity. This repulsion, however, is not enough to create an attractive potential sufficiently strong to bind an electron, as was suggested in a linear treatment of the screening.

The results for a positive impurity are quite different. In marked contrast to the situation in 3D, we find that the screened potential for a proton supports a bound state even in the high-density limit. This result would invalidate the applicability of perturbation theory in this limit. We prove, however, that the results of linear theory are in fact correct even though bound states exist. These results find application in a variety of problems, such as charged impurity scattering and the stopping power of charged projectiles, we also calculated. ■

In a two-dimensional electron gas, a proton can bind two electrons even in the high density limit.

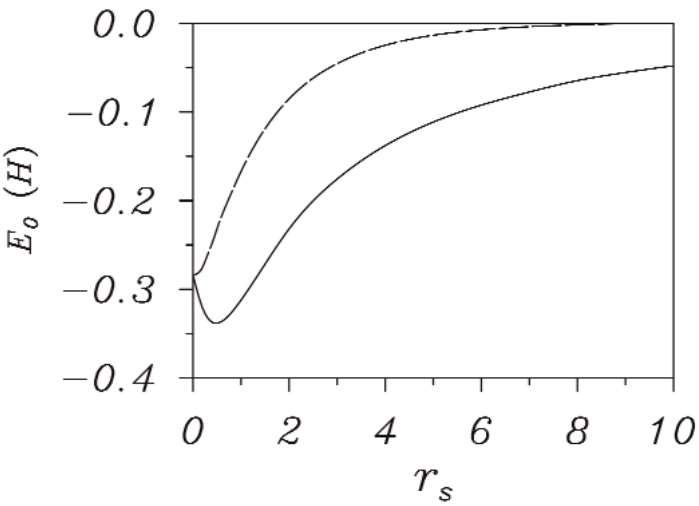

Fig. 2. Bound state eigenvalue for a proton as a function of the 2D electron gas density

REFERENCE
"Nonlinear Screening in Two-Dimensional Electron Gases", E. Zaremba, I. Nagy, and P.M. Echenique, Physical Review Letters **90**, 046801 (2003)

DIPC Highlight

Non-gaussian Nature of the α-relaxation of Glass-forming Systems*

by *J. Colmenero[1,2,3], A. Arbe[2], F. Alvarez[1,2], M. Monkenbusch[4], D. Richter[4], B. Farago[5] and B. Frick[5]*

Molecular dynamics (MD) simulations on glass forming systems of very different nature (Selenium, ortotherphenyl, water,...) have shown a series of "universal features" for the non-Gaussian parameter $\alpha_2(t)$ corresponding to the self-motion of the atoms in the α-relaxation regime. A combination of MD-simulations and neutron scattering on polyisoprene has allowed us to establish that the above mentioned "universal features" of $\alpha_2(t)$ can also be found in glass-forming polymers, and are nicely captured by a simple anomalous jump diffusion model with a distribution of jump lengths.

How do atoms move during the structural relaxation? Key to understand the glass transition!

One of the most intriguing problems in condensed matter physics is the glass transition phenomenon, caused by the freezing of the structural (α) relaxation in a glass-forming system. Therefore, the understanding of the molecular motions during this relaxation is of utmost importance to shed some light on the glass formation process. Neutron scattering (NS) and Molecular Dynamics (MD) simulations are essential for this goal. During last years, extensive NS investigations of the incoherent scattering function $F_s(Q,t)$ have established a universal behaviour for the self-atomic motions in the α-relaxation regime of glass forming systems including polymers. As Figure 1 evidences, $F_s(Q,t)$ shows a stretched exponential functional form characterized by the exponent β:

$$F_s(Q,t) \propto \exp[-(t/\tau_w)^{\beta}] \quad (1)$$

with a characteristic time τ_w that clearly depends on Q, $\tau_w(Q)$. This observation implies the diffusive nature of the atomic motions in this regime. Further-more, in the Q-regime approx. $0.2 \le Q \le 1.5$ Å^{-1} the Q-dependence of τ_w in polymers can be described as $\tau_w(Q) \propto Q^{-2/\beta}$ (inset of Fig. 1), implying a Gaussian form of $F_s(Q,t)$ with negligible values for the non-Gaussian parameter $\alpha_2(t)$.

This is in apparent contradiction to results from MD-simulations on glass forming systems other than polymers. There, $\alpha_2(t)$ shows a maximum that increases with decreasing temperature and shifts according to the thermal behaviour of the structural relaxation time. Thus the question arises: Do glass forming polymers behave in a different way? To answer this question we decided to take a twofold approach: we performed fully atom-

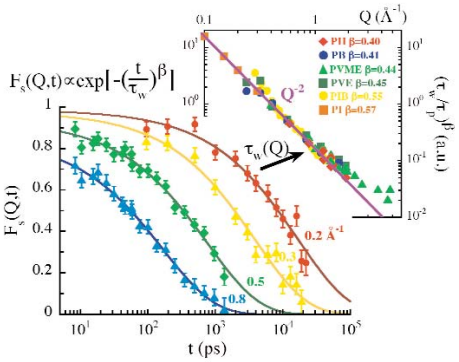

Figure 1: $F_s(Q,t)$ measured on PI at 340 K. Solid lines: fits with Eq. (1). Inset: master curve giving the Q-dependence of τ_w^{β} built with results from six different polymers (see legend), applying polymer-dependent normalising factors (t_p). Solid line: Gaussian behaviour.

1 Departamento de Física de Materiales UPV/EHU, San Sebastián 2 Unidad de Física de Materiales CSIC-UPV/EHU, San Sebastián 3 Donostia International Physics Center, San Sebastián 4 Institut für Festkörperforschung, Forschungszentrum Jülich, Germany 5 Institut Laue-Langevin, Grenoble, France

istic MD-simulations and NS measurements on the same polymer, polyisoprene (PI) [1]. Figure 2 shows the obtained Q-dependence of τ_w. An impressive agreement is found between both kinds of results, validating the MD-simulations. The data univocally confirm the Gaussian-like behaviour in the Q-range approx. $Q \leq 1$ Å^{-1}, while clear signatures of deviations become evident at higher Q-values.

Having established confidence on the realism of our MD-simulations, we can take advantage of them and compute magnitudes that are not easily experimentally accessible, like $\alpha_2(t)$ and the mean squared displacement $\langle r^2(t)\rangle$ of the main chain protons. They are shown in Fig. 3(a), while Fig. 3(b) displays the calculated $F_s(Q,t)$ for several Q-values. As reported for the other glass-forming systems, a main maximum is indeed found for $\alpha_2(t)$ at $t^* \approx 4$ps, just in the early stages of the decaging process identified with the α-relaxation. The shadowed area in Fig. 3 shows the region where $\alpha_2(t)$ takes significant values. For low Q-values this area only covers the initial part of the slow decay (α-regime) of $F_s(Q,t)$. However, as Q increases, the marked time range starts to cover almost completely the slow decay. This naturally explains the finding of the deviations from Gaussian behaviour of $F_s(Q,t)$ at high Q-values. What could be the origin of such deviations? The way the characteristic time departs from the Gaussian expectation (Fig. 2) strongly reminds us on the very well known manifestations of the discrete nature of diffusion in simple jump diffusion models. Basing on this similarity, we have proposed a model that considers a distribution of elementary jump lengths underlying the anomalous diffusion undergone by the atoms in the α-process [1]. Such an extremely simple approach allows a very accurate description of the Q-dependence of τ_w (Fig. 2). The associated distribution of jump lengths $f(\lambda)$ (inset of Fig. 2) shows a maximum at about 0.4 Å. This model also semiquantitatively reproduces the behaviour of $\alpha_2(t)$ [see Fig. 3(a)], within its range of validity (above 1 ps approximately) [1]. It is finally noteworthy that the main "universal features" reported in the literature for $\alpha_2(t)$ are also naturally deduced in this approach [1]. This suggests that the essence of the universal deviations from Gaussian behaviour in the self-motions of atoms during the structural relaxation regime lies in the distribution of discrete steplengths underlying the anomalous diffusion. ■

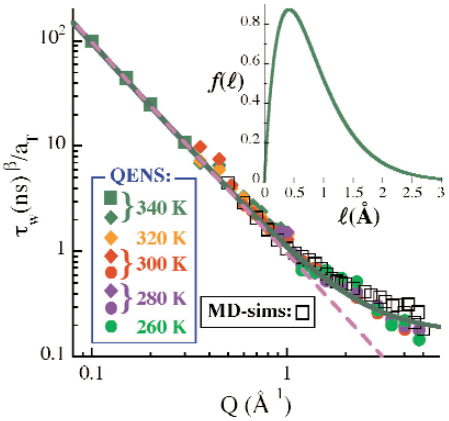

Figure 2: Master curve constructed combining NS and MD-simulations results for PI. T-dependent shift factors a_T have been applied. Dashed line: Gaussian prediction; solid line: description in terms of the anomalous jump diffusion model with the distribution of jump lengths shown in the inset.

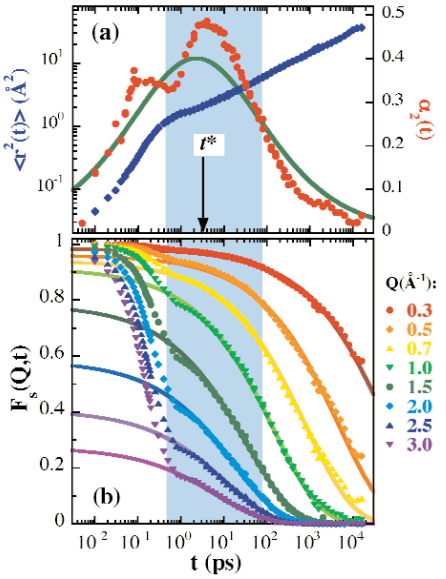

Figure 3: MD-simulations results for PI: (a) Time evolution of $\langle r^2(t)\rangle$ (◆) and $\alpha_2(t)$ (●). Solid line: anomalous jump diffusion model prediction for $\alpha_2(t)$. (b) Fs(Q,t). Solid lines: fits with Eq. (1) ($t \geq 5$ ps). The shadowed area covers the time range of the full-width at half-maximum of the main peak of α_2.

We find polymer behavior similar to other glass forming systems

Non-Gaussian behavior seems to reflect the discrete nature of the motions underlying the structural relaxation

*An extended version of this paper has also been recently published in the MODELLING section of the Scientific Highlights of the 2003 ANNUAL REPORT of the Institut Laue-Langevin (ILL), Grenoble (France)

REFERENCE

[1] A. Arbe, J. Colmenero, F. Alvarez, M. Monkenbusch, D. Richter, B. Farago and B. Frick, Physical Review Letters **89** (2002) 245701; Phys. Rev. E **67** (2003) 51802

DIPC Highlight

Chain Connectivity and Segmental Dynamics of Miscible Polymer Blends

by *E. Leroy*[3], *A. Alegría1*,[2] *and J. Colmenero*[1,2,3]

We have experimentally demonstrated the ability of the effective concentration concept to quantitatively predict the component dynamics in three model miscible polymer blends.

Polymer blending is a convenient way for obtaining new materials with tailor made properties.

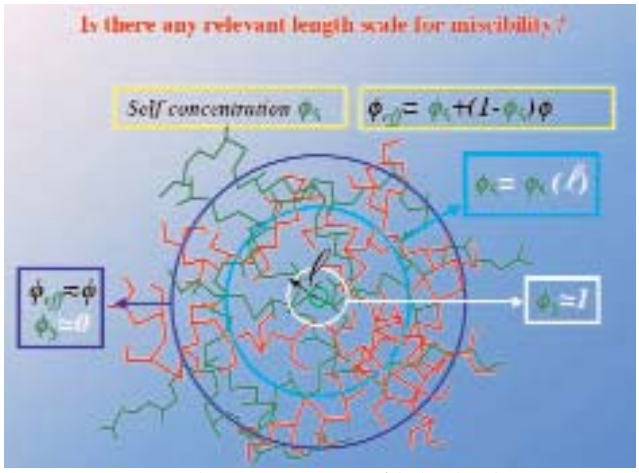

Figure 1: Schematic representation of the length scale dependence of the effective concentration.

Polymer materials, usually referred to as plastics, are found everywhere in the normal life. A route used to obtain new polymer materials is by combining already existing polymers, which allows tuning the desired properties of the resulting material. Among the broad range of multicomponent polymer materials, a family of both, fundamental and technological interest is that of the binary miscible polymer blends. These systems are homogeneous mixtures of macromolecular chains of two types. However, they present what is referred to as dynamical heterogeneity, i.e., the motions of the segments of the two polymer components occur with significantly different time scales. A way to understand the dynamic heterogeneity of miscible polymer blends is to consider the chain connectivity effects. In a miscible polymer blend A/B, the chain connectivity imposes that the local environment of a segment for instance of polymer A is (on average) necessarily richer in this component as compared to the bulk mean composition . Thus, the more flexible component of the blend will move faster than the more rigid one despite the system is miscible. To account quantitatively for this effect, the concept of effective local concentration has been introduced. The effective local concentration sensed by a polymer component, can formally be expressed as:

$$_{eff} = _{S} + (1 - _{S}) \quad \text{eq.1}$$

being $_{S}$ the so called "self-concentration" of the polymer segment considered. Obviously, the value of $_{eff}$ depends on the considered length scale, approaching unity for very short length scales and the average concentration, , for large length scales (see figure 1). Recently, it has been proposed that the relevant length scale for the polymer segmental dynamics (the molecular motions responsible of the glass transition phenomenon) is the Kuhn length (l_K), defined as the length along the chain contour that makes the orientation of a given chain bond to be independent of the orientation of the chain bond at the origin. On the basis of this assumption $_{S}$ can be calculated as the concentration of monomers of a given chain component within a volume $V \sim l_K^3$ centered in a segment of the same chain.

The existence of two different segmental dynamics in a miscible blend would imply the presence of two distinctive glass transition processes — and therefore they should

1 Departamento de Física de Materiales UPV/EHU, San Sebastián 2 Unidad de Física de Materiales CSIC-UPV/EHU, San Sebastián 3 Donostia International Physics Center, San Sebastián

depict two glass transition temperatures, T_g-each associated to one of the two polymer components. The way that has been proposed to calculate these effective glass transition temperatures $T_{geff}(\ )$ for each component in the blend is to use the concentration dependence of the macroscopic (average) glass transition temperature $T_g(\ )$, as measured in a standard differential scanning calorimetric (DSC) experiment, according to the following relationship:

$$T_{geff}(\ )=T_g(\ _{eff}) \quad \text{eq.2}$$

Dielectric measurements on miscible polymer blends can be used to investigate selectively a single component if the other does not contribute to the dielectric relaxation process. Taking advantage of this capability, in this work[1] we have tested in a quantitative way the accuracy of the effective concentration approach above described to account for the dynamical heterogeneity of miscible polymer blends.

Three model miscible blends have been studied by combining DSC and Thermally Stimulated Depolarization Current (TSDC). This second technique can be considered as a dielectric sensitive equivalent of DSC and it allows determining the glass transition temperature sensed by the dielectrically active segments present in the polymer blend. The three blend systems studied take profit of this selectivity. In poly(vinyl methyl ether)/polystyrene (PVME/PS), only the lower T_g component (PVME) is dielectrically active. In polystyrene/poly-o-chlorostyrene (PS/PoClS), PoClS is the dielectrically active and the highest T_g component. Finally, in PVME/PoClS both components are dielectrically active but with a very high T_g difference, which should allow to resolve the corresponding dielectric contributions. DSC measurements showed a single heat capacity step for all blends, confirming their miscibility. Some typical TSDC measurements are illustrated in figures 2. It is apparent that whereas for pure PVME both techniques provide essentially the same value of T_g, for the PVME/PS blends the TSDC peak maximum occurs at a temperature significantly different (lower) than the calorimetric T_g, (middle point of the heat capacity step). The glass transition temperatures obtained for the PVME/PoClS blends using both DSC and TSDC data are plotted on figure 3. To have a quantitative test of the "effective concentration" approach, for each

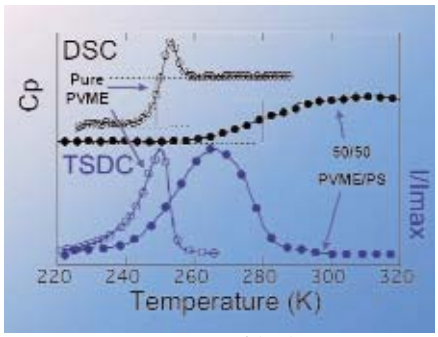

Figure 2: Determination of the glass transition temperatures. DSC: macroscopic T_g and TSDC: T_{geff} of the dielectrically active component.

Two different segmental dynamics would imply two distinctive glass transition temperatures.

blend system, we first fitted the concentration dependence of the bulk glass transition temperature measured by DSC. In a second step, we calculated the corresponding values of T_{geff} of the dielectrically active component according to eq 2. A remarkably good quantitative agreement between the experimental values and the calculated T_{geff} curves can be observed for all measured blends (see Fig. 3). This result demonstrates the ability of the effective concentration approach to account quantitatively for the dynamical heterogeneity of miscible polymer blends. Furthermore, this good agreement pointed out to l_k as the relevant length scale for the glass transition phenomenon in polymers, i.e. a few nanometers, which is much shorter than that commonly assumed. ■

Dielectric techniques allow us to investigate selectively the dynamics of a single component in blend systems.

REFERENCE

[1] E. Leroy, A. Alegría, and J. Colmenero Macromolecules **35**, 5587 (2002)

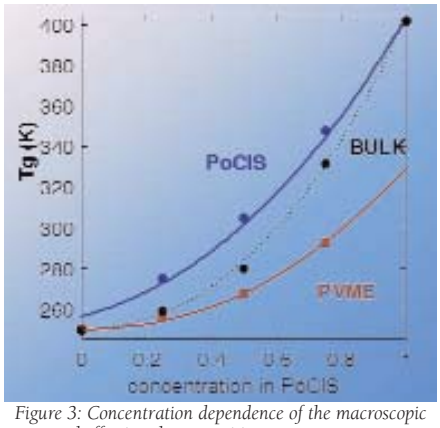

Figure 3: Concentration dependence of the macroscopic and effective glass transition temperatures on PVME/PoClS blends. The lines for the effective glass transition temperatures of the two components (solid lines) were obtained from that of the macroscopic $T_g(\ )$ (dotted line) using eq. 2.

The effective concentration concept captures quantitatively the dynamical heterogeneity of miscible polymer blends.

DIPC Highlight

Crossover from α-relaxation to Rouse Dynamics

by *A. Arbe1, J. Colmenero[1,2,3], D. Richter[4], M. Monkenbusch[4], L. Willner[4], B. Farago[5]*

We report on a large experimental effort exploring the dynamics of poly(vinyl ethylene) on length scales covering Rouse dynamics and below. The results establish for the first time the simultaneous existence of a generic sublinear diffusion regime which underlies the α-process in addition to the Rouse process. Both regimes are separated by a well defined dynamic cross over. From that the size of the Gaussian blobs making up the Rouse model is determined directly. The glassy dynamics is identified as subdiffusive motions occurring within these Gaussian blobs.

Is it possible to experimentally clarify the independent existence of a generic dynamic regime of sublinear diffusion associated with the α-process aside the Rouse process?

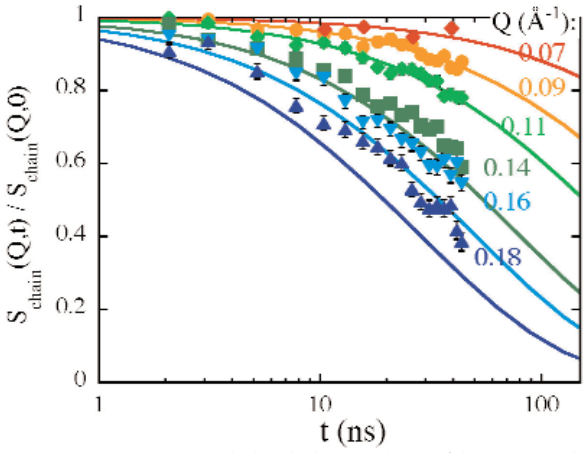

Figure 1. $S_{chain}(Q,t)$. Solid lines: prediction of the Rouse model.

Neutron Spin Echo gives the answer: It is!

Polymers show at the same time the general properties of glass forming systems — with the α-relaxation as the most relevant dynamical process —and features arising from their chain-like nature— the chain motions are described by the Rouse model, that treats the dynamics of a Gaussian chain (beads and springs) in a heat bath.

For a large number of polymers, neutron scattering studies performed at time scales close to the structural relaxation time t_s and in the Q-range 0.2 Å^{-1} ≤ Q approx. have shown that the protons perform sublinear diffusion with a mean-square displacement (msd) $\langle r^2(t)\rangle \sim t^{\beta}$ (β: stretching exponent, $0.4 \leq \beta \leq 0.6$) [1]. This behavior is similar to that predicted by the Rouse model ($\langle r^2(t)\rangle \sim t^{0.5}$). On the other hand, molecular dynamics (MD) simulations [2] and Mode Coupling Theory (MCT) calculations [3] on coarse-grained polymer models (bead and spring models) show the existence of a subdiffusive regime ($\langle r^2(t)\rangle \sim t^{x}$, $x \approx 0.5$-0.6) after the plateau reflecting the "cage effect". This regime was related to the Rouse dynamics of polymer chains. Furthermore, also quasielastic neutron scattering experiments on glass forming polymers taken at high Q were interpreted in terms of Rouse motion [4]. However, in real polymers the precondition of Gaussian beads can only be fulfilled on larger scales. The question thus arises: is it possible to experimentally clarify the independent existence of a generic dynamic regime of sublinear diffusion associated with the α-process aside the Rouse process?

We have performed Neutron Spin Echo (NSE) measurements on the single chain dynamic structure factor $S_{chain}(Q,t)$, related to the collective segment motion within one chain, and the self correlation function $S_{self}(Q,t)$, originated from the proton self motion, for poly(vinyl ethylene) (PVE). The

1 Departamento de Física de Materiales UPV/EHU, San Sebastián 2 Unidad de Física de Materiales CSIC-UPV/EHU, San Sebastián 3 Donostia International Physics Center, San Sebastián 4 Institut für Festkörperforschung, Forschungszentrum Jülich, Germany 5 Institut Laue-Langevin, Grenoble, France

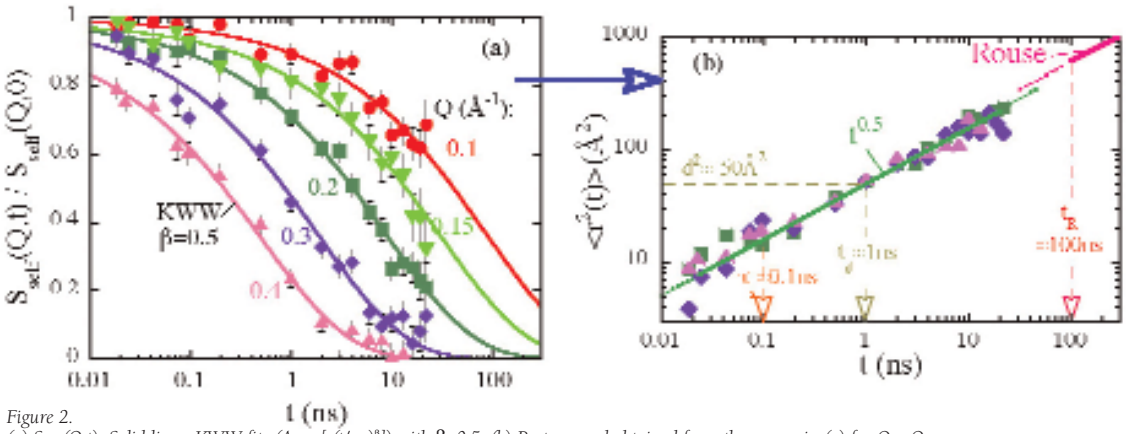

Figure 2.
(a) $S_{self}(Q,t)$. Solid lines: KWW fits ($Aexp[-(t/\tau_w)^\beta]$) with β=0.5. (b) Protons msd obtained from the curves in (a) for $Q > Q_R$.

instruments used were IN15 (ILL) and the NSE spectrometer at the FRJ-2 (Jülich). For a first time we have been able to distinguish clearly two separated dynamic regimes of sublinear diffusion [5].

Figure 1 compares the experimental $S_{chain}(Q,t)$ with the Rouse prediction. For small Q the data follow well the theory. Thus, in this Q-range the particles within the chain perform sublinear diffusion: $\langle r^2(t)\rangle \sim t^{0.5}$. However, at the highest Q's investigated ($Q > Q_R = 0.11$ Å^{-1}) severe deviations are evident (see the figure).

Turning to $S_{self}(Q,t)$ (Figure 2(a)), we can proof the existence of a second Gaussian subdiffusive regime at short length scales by the construction of a Q-independent msd [Figure 2(b)] for $Q \geq 0.20$ Å^{-1}. This follows $\langle r^2(t)\rangle \propto t^{0.5}$ (solid line). Thus, for $t < t_R = \tau_w^{Rouse}(Q_R) \approx 100$ ns the data reveal a subdiffusive regime which is obviously distinct from the Rouse process. This regime is indeed that relevant for the α-relaxation: both, τ_s as well as the time a proton moves as far as the average intermolecular distance d, lie in this region (see the figure) [5]. For $t \geq t_R$, the mean squared displacements follows the Rouse prediction $\langle r^2(t)\rangle^{Rouse}$.

The cross over between the Rouse- and the subdiffusive α-regime becomes most clear if we focus on the Q-dependent characteristic relaxation times (Figure 3). The two regimes are separated by a step at $Q_c \approx 0.13$ Å^{-1}. A cross over length scale $l_c \approx \pi/Q_c = 24$ Å may be obtained, that would be identified with the size of a Gaussian blob underlying the Rouse model. For PVE this corresponds to about ten monomers or twenty bonds. The α-process evolves then from the motion of the atoms within the polymer which are subject to specific intra- and inter-molecular forces. The coarse grained MD-simulations and MCT calculations based on bead and spring models [2,3] do not reveal this α-regime, since it appears to relate to the internal dynamics within the Gaussian blobs. ■

A cross over length scale lc ≈ 24 Å (≈ ten monomers) defines the size of a Gaussian blob underlying the Rouse motion. The α-process relates to the internal dynamics within the blobs.

REFERENCES

[1] Colmenero, J; Alegría, A; Arbe, A; Frick, B. Physical Review Letters 1992, 69, 478.

[2] Binder, K; Baschnagel, J; Paul, W. Prog. Polym. Sci. 2003, 28, 115.

[3] Chong, S.H; Fuchs, M. Physical Review Letters 2002, 88, 185702.

[4] Allen, G; Higgins, J.S; Macounachie A; Ghosh, R.E. Chem. Soc. Faraday Trans. II 1982, 78, 2117.

[5] Richter, D; Monkenbusch, M; Willner, L; Arbe, A; Colmenero, J; Farago, B. Europhysics Letters 2004, 66, 239.

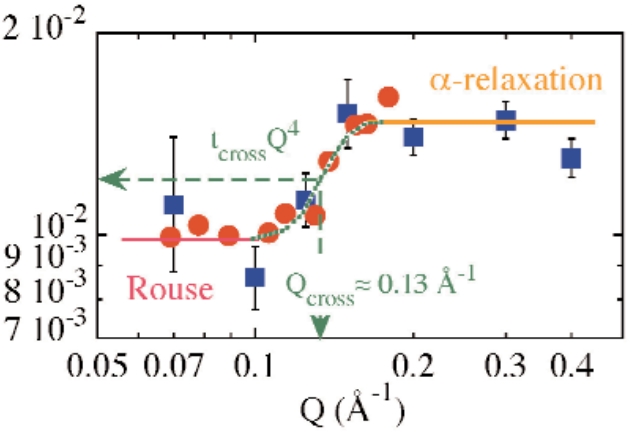

Figure 3. $\tau_w Q^4$ from $S_{self}(Q,t)$ (full squares) and deduced from $S_{chain}(Q,t)$.

DIPC Highlight

Rings Dancing in The Disorder*

by *S. Arrese-Igor[1], A. Arbe[2], J. Colmenero[1,2,3], A. Alegría[1,2] and B. Frick[4]*

By means of quasielastic neutron scattering we have studied the phenylene rings' dynamics in the engineering thermoplastic polysulfone in the glassy state. The wide dynamic range covered has allowed us to identify the simultaneous occurrence of fast oscillations and π-flips. A model combining these two motions nicely describes the results in the whole dynamic range investigated. The structural disorder characteristic of the amorphous state leads to broad distributions of characteristic times.

Understanding the molecular motions underlying secondary relaxations in polymers can help to design materials with tailor made properties.

Have you ever realized the importance of plastics in your daily life? Look around. You can find them in your computer, printer, furniture, car,...everywhere. This is because they are durable, light, cheap, and their good mechanical and thermal properties make them suitable for a huge number of applications. Engineering thermoplastics like polycarbonate or polysulfone have for these reasons a salient important technological significance. Their interesting ultimate mechanical properties are probably related to the ability of these polymers to accommodate a stress with highly activated molecular motions, in these cases likely involving π-flips of their phenylene rings. That is why considerable efforts have been made to identify the molecular origin of the so called secondary relaxations in polymers. Though the existence of these processes and their main general features are established for many decades, their microscopic origin remains elusive. This is due to the fact that they have traditionally been studied by relaxation techniques like Mechanic (MS) and Dielectric (DS) Spectroscopy that do not provide microscopic information and space resolution. On the other hand, the few existing Neutron Scattering (NS) studies on the molecular motions behind the secondary relaxations in polymers have been performed close or above the glass transition temperature T_g, where the main α-relaxation is also active.

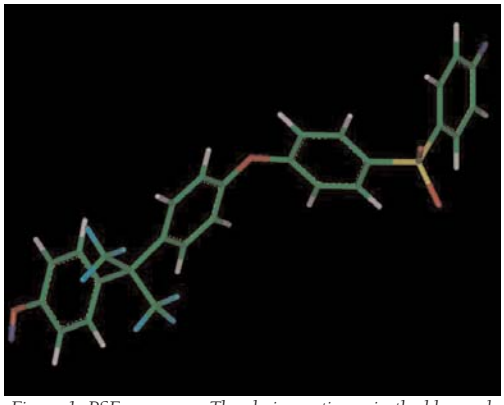

Figure 1. PSF monomer. The chain continues in the blue ends.

Here we have exploited NS capabilities for deciphering the microscopic motions undergone by polysulfone phenylene rings deep in the glassy state with a twofold aim: contribute to the fundamental question about the origin of secondary relaxations in polymers and provide useful information for further design of plastics with tailor made mechanical properties.

The measurements were performed at the Institute Laue-Langevin (ILL) on polysulfone (T_g = 460 K) with deuterated methyl groups (Figure 1), covering the micro- (≈ 0.1 ps to 20 ps) and mesoscopic (≈ 100 ps to 1 ns) timescales. The spatial resolution of NS techniques has been exploited to identify the nature of the dynamical processes detected. The geometry of the motions involving

1 Departamento de Física de Materiales UPV/EHU, San Sebastián 2 Unidad de Física de Materiales CSIC-UPV/EHU, San Sebastián 3 Donostia International Physics Center, San Sebastián 4 Institut Laue-Langevin, Grenoble, France

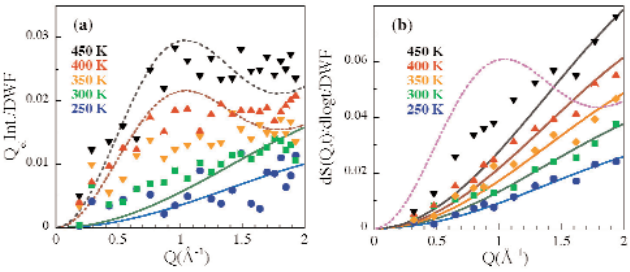

Figure 2: Q-dependence of the magnitudes reflecting the geometry of the motion in the mesoscopic (a) and microscopic (b) timescales. Lines indicate the expectation for jumps of the aromatic protons between two equivalent positions separated a distance d= 4.3 Å (dashed lines) and d= 1.5 Å (solid lines).

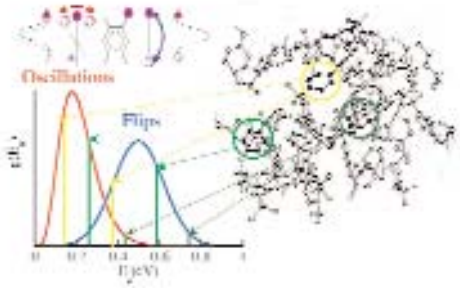

Figure 3: Activation energy distributions for the flip and oscillatory motion.

phenylene rings can be envisaged through the Q-dependence of the scattered intensities. As commented above, a movement that is suspected to occur is a π-flip of the phenylene ring. Then the motion of the aromatic hydrogens would correspond to a jump over two equivalent positions separated by 4.3 Å, leading to a maximum in the quasielastic intensity at about 1 $Å^{-1}$. Is this expectation realized in our experiments? Look at Figure 2. For the highest temperatures investigated, the motion observed in the mesoscopic window indeed corresponds to such a flip. However, on the other extreme, the lowest temperatures showing relaxational features on the microscopic window display a completely different Q-modulation, that would reflect a much more restricted motion in space (amplitudes of ≈ 1.5 Å). This dynamical process might be interpreted as phenylene ring small angle oscillations around the main chain axis, and clearly dominates in the microscopic window. However, with increasing temperature contributions of the π-flips also appear there (see the clear "bump" at 450 K). In a similar way, at mesoscopic scales the high Q-intensity resolved at T ≤ 300 K indicates the contribution of the small amplitude motions. Thus, both processes contribute to both windows. A global description considering the two motions is necessary to reproduce the experimental results in the full dynamic range investigated.

A model considering statistically independent π-flips and small angle oscillations for phenylene ring motion [1] allows a nice description of the experimental observations. Reflecting the effect of disorder in these relaxation mechanisms, broad distributions of activations energies have to be invoked (Figure 3). They are originated by the packing heterogeneity characteristic for the amorphous nature of polymers. The mean activation energy value obtained for the flips, ≈ 0.43 eV, agrees well with that found by spectroscopic techniques in similar systems for the secondary γ-relaxation—responsible for the good mechanical properties. On the other hand, the oscillations show an amplitude that increases with temperature and a mean activation energy, about 0.2 eV, close to that determined for methyl group rotations by NMR and the δ-relaxation by MS. In the proposed scenario, the apparent activation energy for flips would represent a real potential barrier over which the phenylene ring jumps. In contrast, oscillations would take place – probably correlated with other fast motions with small associated spatial scales like methyl group rotations — as a result of rapid fluctuations of the single particle potential seen by the phenylene ring, and produced by the surrounding atoms. In this case, the apparent activation energy for oscillations would only reflect the characteristic time of such fluctuations.■

Neutron scattering allows to identify two kinds of motion for phenylene rings

Disorder leads to broad distributions of barriers

The microscopic motions here unveiled seem to be responsible for the secondary relaxations observed by spectroscopic techniques

*An extended version of this paper has also been recently published in the SOFT MATTER section of the Scientific Highlights of the 2003 ANNUAL REPORT of the Institut Laue-Langevin (ILL), Grenoble (France)

REFERENCES

[1] S. Arrese-Igor, A. Arbe, A. Alegría, J. Colmenero and B. Frick, J. Chem. Phys. 120, 423 (2004)